Journal of
Manufacturing and Materials Processing

MDPI

Article

Investigations on the Influences of the Thermomechanical Manufacturing of Aluminium Auxiliary Joining Elements

Thomas Borgert *, Maximilian Henke and Werner Homberg

Forming and Machining Technology, Paderborn University, Warburger Straße 100, 33098 Paderborn, Germany
* Correspondence: tb@luf.upb.de

Abstract: The demands on joining technology are constantly increasing due to the consistent lightweight construction and the associated increasing material mix. To meet these requirements, the adaptability of the joining processes must be improved to be able to process different material combinations and to react to challenges caused by deviations in the process chain. One example of a highly adaptable process due to the two-step process sequence is thermomechanical joining with Friction Spun Joint Connectors (FSJCs) that can be individually adapted to the joint. In this paper, the potentials of the adaption in the two-stage joining process with aluminium auxiliary joining elements are investigated. To this end, it is first investigated whether a thermomechanical forming process can be used to achieve a uniform and controlled manufacturing regarding the process variable of the temperature as well as the geometry of the FSJC. Based on the successful proof of the high and good repeatability in the FSJC manufacturing, possibilities, and potentials for the targeted influencing of the process and FSJC geometry are shown, based on an extensive variation of the process input variables (delivery condition and thus mechanical properties of the raw parts as well as the process parameters of rotational speed and feed rate). Here it can be shown that above all, the feed rate of the final forming process has the strongest influence on the process and thus also offers the strongest possibilities for influencing it.

Keywords: joining; aluminium; friction; forming; reliability

Citation: Borgert, T.; Henke, M.; Homberg, W. Investigations on the Influences of the Thermomechanical Manufacturing of Aluminium Auxiliary Joining Elements. *J. Manuf. Mater. Process.* **2023**, *7*, 147. https://doi.org/10.3390/jmmp7040147

Academic Editor: Paulo A. F. Martins

Received: 14 July 2023
Revised: 7 August 2023
Accepted: 9 August 2023
Published: 10 August 2023

1. Introduction

Current global challenges require the optimisation of energy and resource efficiency of conventional vehicles, facilities, and production processes. One example of a sector in which energy and resource efficiency is becoming increasingly important is the automotive industry [1]. With the consistent lightweight construction of vehicles, resources can be saved on the one hand during production. In addition, fuels and emissions can also be reduced during the vehicle's use phase [2,3]. Taking consistent lightweight construction into account, a variety of different construction materials such as high-strength steels, aluminium, and fibre-reinforced plastics are used, resulting in a multi-material mix [4,5]. The use of fibre composites in particular is increasing, which brings new challenges for joining technology [6]. Thermal joining by welding of dissimilar material pairings is very challenging and, in some cases, not even possible [7]. One possibility to thermally join dissimilar metallic material pairs is the use of resistance spot welding (RSW) [8]. Despite the fact that dissimilar metallic material pairs (such as aluminium and steel) can be joined with this process, some challenges remain as the incompatible thermo-physical properties such as melting temperature, different coefficient of thermal expansion and thermal conductivity, along with the formation of brittle intermetallic compound (IMC) [9]. Investigations show that the joining of non-metallic components (such as fibre-reinforced plastics) with steels is also possible [10,11]. However, this usually requires complex process alternatives of resistance spot welding, which lose their adaptability accordingly.

To overcome some of the challenges of the thermal joining processes, mechanical joining methods such as self-pierce riveting or mechanical clinching have been increasingly used in recent years [12,13]. The investigations of the past years on the mechanical joining processes show that due to the manifold influencing variables, the most different material combinations can be joined, but also the extensive influences of the process parameters have to be researched [14,15]. The versatile joining of different material combinations can be implemented by different mechanical joining processes with and without auxiliary joining elements [12,16]. Each of the joining processes has separate requirements for the joining partners or the accessibility of the joining point [17]. A prerequisite for clinching, for example, is sufficient ductility of the materials to be joined, which significantly reduces the range of materials to be processed and increases the risk of cracks occurring in materials with low ductility [18]. Another limitation of mechanical joining processes (such as, e.g., self-piercing riveting) can be the fact that the fibre structure of fibre-reinforced plastics is damaged during joining by the forming of the sheet materials [19].

One possibility to overcome the challenges described above, i.e., the lack of ductility of the sheets to be joined and the lack of transformability, is the use and formation of an auxiliary joining element in the direct vicinity of the joining process. Thermomechanical joining processes, which are characterised by the combination of mechanical and thermal treatment of the material to be formed, are suitable for this purpose [20]. One example of a thermomechanical joining process with an auxiliary joining element and accessibility only required on one side is flow drilling screwing [21]. This process uses a rotating bolt-shaped auxiliary joining element to form a thread in the resulting draft [22]. Due to the frictional contact as well as the relative speed between the sheets and the auxiliary joining element, heat is generated, the flow stress of the sheets to be formed is reduced and thus the process supports the forming of the draft [23,24]. Challenges are posed by the need for auxiliary joining elements specially adapted to the joint in advance as well as the limited joinability of thin sheets due to the necessity of forming a thread. A thermomechanical joining process that does not require an auxiliary joining element is friction stir welding [25]. In this process, friction and thus heat are generated by the contact of the rotating die with the joining partners, the sheets are plasticised, and a joint is created [26,27]. Due to the low process temperature compared to conventional welding methods, friction stir welding has several advantages, such as the elimination of the need for post-processing [25]. Nevertheless, the strength of the joint depends on the process parameters used and, above all, on a suitable process temperature [28]. Despite the extensive advantages, the limitation remains that the connection between the materials is only realised by the material bond. Comparatively high forces occur in the process and the arrangement of the joining partners and the design of the joint itself is limited.

To further improve the adaptability of the thermomechanical joining process and to improve the joint strength by using a form-fit as well as a force-fit, a two-stage thermomechanical joining process with auxiliary joining element has been researched for a few years. In this process, the adaptive auxiliary joining elements are manufactured in a thermomechanical forming process by means of a shaping tool in a first process step depending on the requirements of the joint [29] (explanation of the process principle in Section 2). To date, research has been carried out into the use of aluminium and steel auxiliary joining elements with a wide range of geometries and (mechanical) properties to be set in the process [30]. The manufacturing of auxiliary steel joining elements, which has been extensively considered in investigations, enables the (pre-hole-free) joining of a wide range of different material thickness combinations made of aluminium and steel [31]. The feasibility and thus also the high versatility of the thermomechanical joining process with adaptive friction elements has thus been successfully demonstrated in past investigations. A high degree of versatility in the processing of aluminium auxiliary joining elements is provided by the many possibilities of influencing the process parameters such as rotational speed and feed rate while pre-rubbing and forming. The large number of process parameters also leads to

a wide range of influences on the process and the properties of the resulting joint. In this paper, the possibilities for influencing these parameters are examined in detail.

2. Materials and Methods

This section first describes the principles of the thermomechanical forming process of the Friction Spun Joint Connectors (FSJCs) and the possibilities to influence this process, a characterisation and naming of the properties of the semi-finished products used, the experimental plan applied, and the methods and measuring devices for evaluation are described.

2.1. Thermomechanical Forming of the Friction Spun Joint Connectors (FSJCs)

The fundamental idea of the joining process with integrated manufacturing by forming the Friction Spun Joint Connectors is the possibility of adapting the auxiliary joining part geometry to the requirements of the respective joining task. This adaptation can and should take place directly before the actual joint is produced. Based on the extremely high adaptability, the previously described challenges of conventional joining processes regarding the adaptation to different material and material combinations are to be solved. This adaptability to different joining tasks can be achieved by adapting the diameter, the length, and the geometry of the closing head (the parameters are explained later in this section) to the individual auxiliary joining element. The precondition for this adaptation to the geometry is a forming process that provides many degrees of freedom due to its kinematic shape formation. Figure 1a shows the schematic sequence of the thermomechanical forming process to be compared with a picture of the real experimental setup in Figure 1b. The raw shape of the FSJC represents a round bar section that can be used universally and is also readily available. This round bar section is clamped in a collet of a suitable milling machine at the beginning of the first process step (Step I). This horizontally arranged milling spindle from the manufacturer WEISS Spindeltechnologie GmbH, Maroldsweisach (Germany) allows a maximum rotational speed of n_{max} = 15,000 rpm, so that the rotational movement within the forming process is carried out by the workpiece. As a result, only rotationally symmetrical FSJCs can be produced (without a major effort) at the time of this publication. The relative movement necessary to create a user-specific geometry of the FSJC is realised by a cross support (traverse movement in the x- as well as y-direction) to which the die is attached. Two different process control strategies can be used to manufacture the FSJC. On the one hand, heat can first be selectively applied into the workpiece with the (carbide) tool by means of a frictional contact on the face of the die with the round bar section (Step II). Following this pre-rubbing step, the actual FSJC geometry is manufactured (Step III). For the second process control strategy, the process of pre-rubbing can also be omitted and the FSJC can be produced directly by means of the forming process (Step III). Following the forming process, the properties of the FSJC can still be adapted to the requirements of the joining point by means of a machining reworking process (adaptation of the geometry by e.g., grinding or machining) and the mechanical properties can be adapted to the requirements of the joining point by quenching (particularly relevant for steel materials) (Step IV) [31].

2.2. Characterisation of the Workpieces and Dies Used

Each of the round bar sections used in the following investigations has a diameter of d_0 = 8 mm, a length of l_0 = 35 mm, and is made of the wrought aluminium alloy EN AW-6060. The chemical composition of the aluminium rods used is listed in Table 1. The aluminium rods are delivered in the heat treatment condition T66 (solution annealed and artificially aged with a special control of the process). To assess the influence of the heat treatment condition on the thermomechanical forming process, one half of the round bar sections used are transferred to the heat treatment condition T4 (solution annealed and cold aged). This is done by means of a solution annealing process at a temperature of T = 540 °C (time t = 2 h) in a furnace followed by quenching in a water bath. Due to the

high tool loads associated with the thermomechanical forming process, the tools used for the investigations are made of sintered carbide KX 40 (Co 9%, WC 91%).

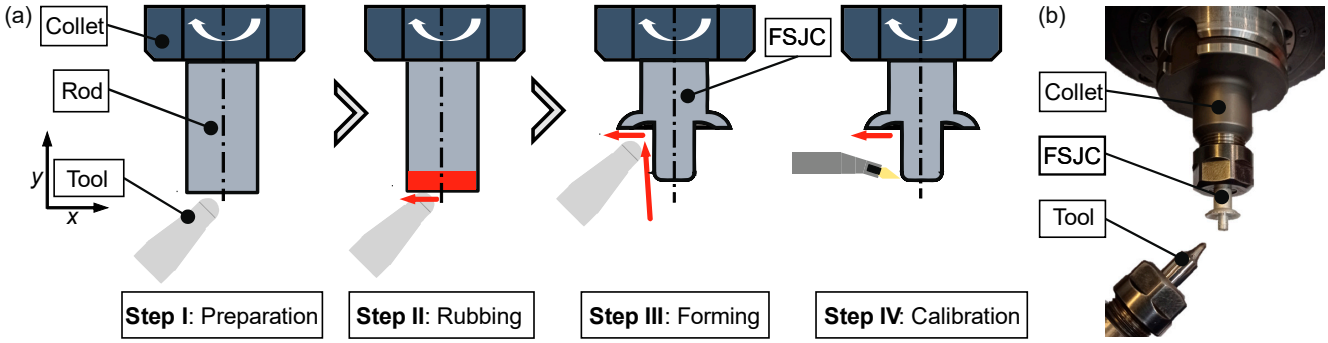

Figure 1. Thermomechanical forming process to manufacture the FSJC, (**a**) process steps, (**b**) picture of the experimental setup.

Table 1. Chemical composition of the EN AW-6060 round bar used in the investigations.

Elements	Al	Fe	Si	Cu	Mn	Mg	Zn	Ti	Cr
Mean value in wt%	Balance	0.17	0.54	0.01	0.03	0.55	0.01	0.01	<0.01

2.3. Experimental Plan

The manufacturing of FSJCs with different dimensions (e.g., from round bars as well as from tubes) has been successfully demonstrated in past investigations. The central object of this investigation is to show the influence of the process parameters of the thermomechanical forming process on the process itself as well as the geometry of the FSJCs. On the process side, the rotational speed of the round bar section as well as the feed rate of the die can be influenced in a wide interval both during the pre-rubbing phase and during the forming phase. Together with the material condition, five factors are varied in a wide spectrum in each case. For the rotational speed in the pre-rubbing process, six points between 0 rpm (no pre-rubbing) and 14,500 rpm are considered as well as six different feed rates between 0 mm/min (no pre-rubbing) and 150 mm/min during pre-rubbing. For the forming process, five rotational speeds between 6000 rpm and 14,500 rpm as well as five feed rates between 25 mm/min and 700 mm/min are considered, which in total represents a wide range of parameters. In addition, the material condition and thus also the mechanical strength and ductility of the raw shapes in the form of the round bar sections are varied between T4 and T66. Due to the high number of experiments that had to be carried out for a full factorial experimental plan, a partial factorial experimental plan is used. For each of the considered experimental points, four additional repeat experiments are carried out, so that a total of 454 experiments are considered for the evaluation. The order of the experiments was randomised.

2.4. Analysis and Evaluation of the Experiments

Five target variables are considered for the following evaluation. The relative weight loss represents a measure of the loss of material, i.e., a cutting removal of material. Due to the optical properties of aluminium, it is not possible to measure the temperature accurately and correctly using a thermographic camera. Instead, a tactile measurement approach with a type K thermocouple, which is located on the stationary die approx. 5.5 mm away from the contact point with the workpiece, is used in the investigations. Due to this indirect measuring principle, the measured temperature serves as a qualitative comparison value, as it will be below the true workpiece temperature. Furthermore, three geometric target values (shown in Figure 2) are considered for the evaluation. To achieve the best possible form fit, the parameters of the undercut u (difference of l_2 and l_1) and the flange diameter

d_f must be maximised. In addition, the shaft diameter of the FSJC d_1 is examined in the evaluation.

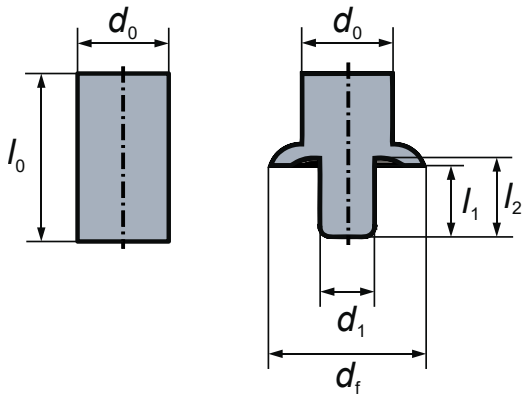

Figure 2. Geometric parameters of the semi-finished products as well as the manufactured FSJC.

3. Results and Discussion

The introduction of this publication motivates research on versatile thermomechanical processes for joining a wide variety of material combinations. Due to the many influencing parameters (e.g., kinematic shape generation or process parameters such as rotational speed and feed rate), extensive basic research into the effects of the individual process parameters must be carried out before industrial application. The results presented in the following are intended to contribute to the understanding of the influencing variables as well as the possibilities for the repeatable manufacturing of FSJCs. For this purpose, the results of the investigations with regard to the repeatability of the FSJC production of a geometry with identical parameters are first discussed. Subsequently, it will be highlighted which process-side influencing factors have the strongest effect on the targeted adjustment of the geometric characteristic values of the FSJCs.

3.1. Evaluation of the Repeatability

The results of the investigations on the repeatability of the manufacturing process of the FSJCs are presented below under the consideration of exemplary series of experiments. For each identical process parameter combination, four additional repetition experiments are carried out. From two series of experiments with a significant different feed rate, one FSJC (raw material condition T66) each is shown (high feed rate in Figure 3a and a low feed rate in Figure 3b to illustrate the influence of the feed during forming. In addition, the mean values and standard deviations of central geometric parameters of the entire test series (consideration of all five FSJC produced) are compared in Table 2. The FSJC produced with the high feed rate shows a flange inclined towards the later joining partner with a positive undercut, which is well suited for achieving a form fit in the joined connection. In comparison, the low feed rate results in an FSJC geometry with a flange inclined towards the collet, which is not well suited for joining. Despite the flange geometry suitable for setting a form fit, the FSJCs produced at a high feed rate show smaller cracks (Figure 3a) over the outer diameter.

Table 2. Central geometric parameters and associated deviations for the entire test series with high as well as low feed rates.

Condition	n_R (rpm)	n_f (rpm)	f_R (mm/min)	f_f (mm/min)	$Ød_F$ (mm)	SD ($Ød_F$)	$Ød_1$ (mm)	SD ($Ød_1$)
T66	0	0	14,500	700	13.2	0.14	5.45	0.03
T66	0	0	14,500	25	12.4	0.13	4.9	0.07

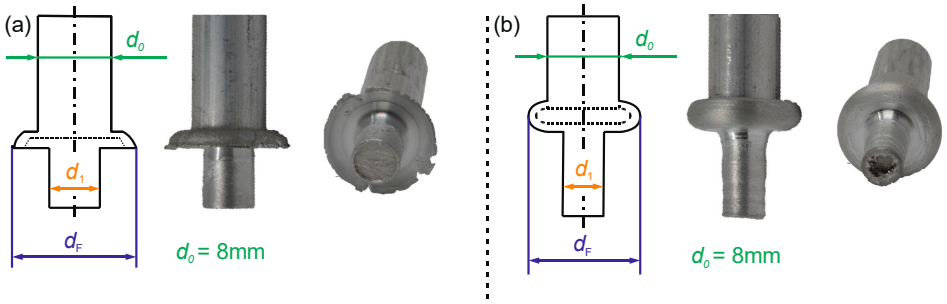

Figure 3. Exemplary illustration of one FSJC (T66) each from two different series of experiments (both $n_R = f_R = 0$, n_f = 14,500 rpm) with (**a**) a high feed rate of f_f = 700 mm/min, (**b**) a low feed rate of f_f = 25 mm/min.

Whether these smaller cracks have an influence on the strength of the later manufactured joint connection or whether they can even have a positive influence as an anti-twist device must be evaluated in future investigations. Regardless of this, such cracks can be removed during the production of the FSJC (analogous to conventional spinning processes) or the formation of the cracks can be avoided by using a counter roll.

In addition to the figure, central geometrical and more detailed results of FSJCs from four series of experiments are presented in Table 3 to mainly show the influence of the material condition. For each delivery state, five FSJCs manufactured with identical process parameters ($n_R = f_R = 0$, n_f = 14,500 rpm, f_f = 700 mm/min) are compared. The mean value of the flange diameter d_f of the as-delivered condition T66 is d_f = 13.2 mm (standard deviation SD = 0.14 mm) which corresponds to 1% (Table 2). For the series of experiments of the condition T4, the mean value of the shaft diameter is d_1 = 5.45 mm (SD = 0.03 mm), which is less than 1%.

Table 3. Almost identical geometries achievable in a series of experiments with high feed rate for the conditions T4 and T66 and compared to very different results for a low feed rate.

FSJC	Condition	n_R (rpm)	n_f (rpm)	f_R (mm/min)	f_f (mm/min)	u (mm)	d_1 (mm)	d_f (mm)
I	T66	0	0	14,500	700	1.05	5.35	13.3
II	T66	0	0	14,500	700	0.95	5.4	13.2
III	T66	0	0	14,500	700	1	5.4	12.95
IV	T66	0	0	14,500	700	1.15	5.45	13.35
V	T66	0	0	14,500	700	1.1	5.5	13.15
I	T4	0	0	14,500	700	0.35	5.4	14.35
II	T4	0	0	14,500	700	0.5	5.45	14
III	T4	0	0	14,500	700	0.55	5.45	13.85
IV	T4	0	0	14,500	700	0.65	5.45	13.85
V	T4	0	0	14,500	700	0.5	5.5	13.8
I	T66	0	0	14,500	25	−4.2	4.9	12.5
I	T4	0	0	14,500	25	−3.6	5.4	12.1

The repeatability results for both delivery conditions manufactured with identical parameter sets are supplemented with one experimental point each with a changed parameter set (here, a low feed rate during forming of f_f = 25 mm/min were used). This shows in this context that with the variation of the process parameters (as well as the delivery condition) significant differences in the geometric parameters can be set, which will be considered in detail in the following subchapter. However, the central findings of the observation of the experiments presented here for the delivery states T4 and T66 remain the high and good repeatability in the manufacturing of FSJC with an identical parameter set. The consideration of further series of experiments (also with identical parameter sets) confirms

the result described before, the good and high repeatability for a series of experiments with identical process parameters.

In addition to the consideration of the geometry, conclusions regarding the uniformity and reproducibility of the FSJC manufacturing process itself can be drawn from the course of the temperature measured at the tool as well as from its maximum value. For this purpose, Figure 4 shows the temperature curves of two different process parameter combinations (high and low feed rate of f_f = 700 mm/min and f_f = 25 mm/min) of three repeat trials each. The pre-rubbing conditions (f_R = 150 mm/min and n_R = 11,625 rpm) are identical and the rotational speed during FSJC forming is comparable (for f_f = 700 mm/min the rotational speed is n_f = 14,500 rpm and for f_f = 25 mm/min the rotational speed is n_f = 12,375 rpm). The first finding shows that in each case the three repeat trials have an almost identical course of the temperature curve (measured on the shaping tool). For the higher feed rate of f_f = 700 mm/min, a higher heating rate (i.e., a steeper increase) can be recorded. Due to the significantly higher feed rate, the process time until reaching the temperature maximum is significantly shorter for the high feed rate. The average maximum temperature of T_{Max} = 222.7 °C (standard deviation SD = 3.2 °C) results for the low feed rate (due to the longer process time) for all three repetition experiments is considered and a temperature of T_{Max} = 122.1 °C (SD = 1.9 °C) for the higher feed rate (due to the significantly shorter process time). In addition to the central finding that a reproducible process is also present with regard to the course and the maximum value of the temperature, the results here confirm that significantly more heat is applied to the workpiece with a lower feed rate. This can be explained by the higher process temperature as well as the higher friction path (at identical rotational speed) at a lower feed rate and thus longer process time. Summarising the investigations described here, it can be highlighted that both the geometry of the FSJC and the measured process variable of the tool temperature show a high and good agreement among the repeated experiments. This is (in addition to the prerequisite for the industrial applicability of this process) also a necessary requirement for the following investigation of the effects and parameter influences of the input variables on the thermomechanical forming process.

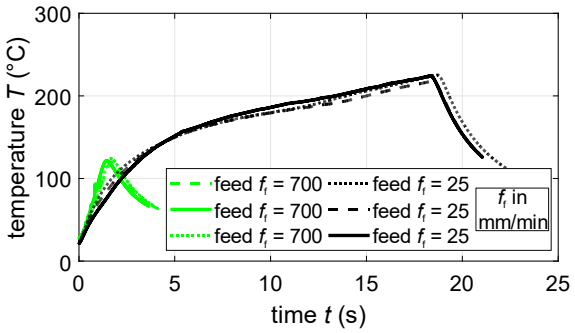

Figure 4. Comparison of the temperature curves of three exemplary repeat experiments for two very different feed rates and otherwise similar parameters.

In addition to directly influencing the process time, the feed rate also influences the amount of heat generated in the process and thus also brought into the FSJC, as already described. The amount of heat brought into the process also changes the properties of the FSJC. When using a low feed rate (e.g., f_f = 50 mm/min), a softening of the FSJC originally in the T66 state takes place. The hardness following the thermomechanical forming process is reduced to H = 50 HV (with an original hardness of H = 90 HV). When using a high feed rate of f_f = 700 mm/min, almost no softening of the FSJC takes place and the original hardness is preserved. It can be assumed that in addition to the mechanical strength, other properties such as ductility or fracture toughness can also be specifically influenced by the process control. Due to these process characteristics, there are further possibilities for the targeted adjustment of central properties, which, however, have a greater potential for FSJC

steel materials compared to aluminium due to the possibilities for pre-hole-free joining by means of driving-through softer sheets. Past investigations were able to demonstrate the targeted hardening of the steel material C45E following the thermomechanical forming process by means of a targeted quenching process [30].

3.2. Evaluation of the Influences of the Process Parameter

Following the result that the manufacturing process of the FSJC is reproducible and the previously considered FSJC show a high agreement of the geometric parameters, it is possible to consider the effects of the different parameters. In addition to the influence of the process parameters (rotational speed as well as feed rate during both pre-rubbing and forming), the delivery condition of the round bar sections is varied to determine the influence of their mechanical properties.

First, the influence of these variables on the process and thus, more precisely, on the maximum tool temperature as well as on the process time, until the maximum temperature is reached, is examined. The influence of the factors described above on the two target values of the maximum temperature and the process time, until the maximum temperature is reached, are shown in Table 4. The effects of the factors are determined based on a multivariate, linear regression model using the software Matlab (R2021b), The MathWorks, Inc. In addition to the coefficients and the *p*-value, the maximum possible effect based on the parameter range examined is also listed in the table. Effects with a *p*-value exceeding the threshold of 5% are marked accordingly and discarded as non-significant results.

Table 4. Effects of the input variables on the maximum die temperature and its time.

Criteria	Value	Constant	n_R	n_f	f_R	f_f	Condition
maximum temperature T_{Max} (°C)	Coefficient	160.6900 °C	0.0037 °C/rpm	-	-	$-0.1477\ \frac{°C*min}{mm}$	−5.8032 °C
	p-value	<5% ✓	<5% ✓	>5% X	>5% X	<5% ✓	<5% ✓
	Max. effect	**-**	**52.9 °C**	**-**	**-**	**−99.7 °C**	**−11.6 °C**
time till T_{Max} (s)	Coefficient	15.8450 s	0.0003 s/rpm	-	$-0.0257\ \frac{s*min}{mm}$	$-0.0213\ \frac{s*min}{mm}$	-
	p-value	<5% ✓	<5% ✓	>5% X	<5% ✓	<5% ✓	>5% X
	Max. effect	**-**	**4.3 s**	**-**	**−3.9 s**	**−14.4 s**	**-**

The central result is that the feed rate during the actual forming of the FSJC has the strongest effect and thus also the strongest influence on the maximum temperature as well as on the time until this is reached. Here, the negative value of the max. effect means in this case that with an increasing feed rate during the forming process, the maximum temperature as well as the process time until reaching it decreases. Furthermore, the rotational speed of the pre-rubbing also shows a significant and thus positive influence on the maximum tool temperature. With the higher rotational speed, the length of the friction path is increased, and thus more energy is applied to the process. The result of the time until the maximum temperature is reached can be used as a kind of control result. A variation of the feed rate is automatically accompanied by a variation of the process time. Due to the identical process sequence for all considered experiments and the symmetrical temperature curve, it can be assumed that the process time, as well as the time until the maximum temperature is reached, correlate. The result that a higher feed rate is accompanied by a shorter process time and thus also time to reach the temperature maximum is therefore in line with expectations (due to the faster tool movement). The tendency for the feed rate during the start-up process to reach the temperature maximum at a lower feed rate at a later point in time can also be seen. Due to the significantly lower proportion of the total process time in relation to demoulding, the effect is smaller.

The effects of the different predictors on the geometric characteristics of the FSJC are shown in Table 5 and explained below. The undercut of the closing head of the FSJC serves to create a form-fit as well as a force-fit connection and is furthermore intended to enable an additional force-fit component for future investigations by means of subsequent pressing. In the case of a positive characteristic value u, a closing head is formed that

is aligned with the upper sheet, which supports the force and form-fit connection. As a quality characteristic regarding the undercut, it can therefore be stated that this should be positive and maximised. Considering the results from the multivariate regression analysis, the significant adjustment of a positive undercut is possible above all when a high feed rate is used during the forming process (the effect which clearly overlays those of the other input variables). The effect of increasing the rotational speed during driving or using the harder material T66 is smaller compared to the effect of the feed rate during forming. The rotational speed during forming has a reverse effect (compared to the rotational speed during driving) and increases the formation of a flange that is inclined to the collet, which is less suitable for the joint.

Table 5. Effects of the input variables on the geometry of the FSJC.

Criteria	Value	Constant	n_R	n_f	f_R	f_f	Condition
undercut u	Coefficient	−0.56886 mm	0.00004 mm/rpm	−0.00007 mm/rpm	-	0.00311 min	0.34449 mm
	p-value	<5% ✓	<5% ✓	<5% ✓	>5% X	<5% ✓	<5% ✓
	Max. effect	**-**	**0.65 mm**	**−0.63 mm**	**-**	**2.10 mm**	**0.69 mm**
relative weight loss	Coefficient	1.999%	−0.00006 %/rpm	0.00008 %/rpm	-	0.004807 $\frac{\% * \text{min}}{\text{mm}}$	-
	p-value	<5% ✓	<5% ✓	<5% ✓	>5% X	<5% ✓	>5% X
	Max. effect	**-**	**−0.92%**	**0.67%**	**-**	**3.24%**	**-**
shaft diameter d_1	Coefficient	5.4338 mm	-	-	0.00072 min	0.00011 min	0.17599 mm
	p-value	<5% ✓	>5% X	>5% X	<5% ✓	<5% ✓	<5% ✓
	Max. effect	**-**	**-**	**-**	**0.11 mm**	**0.07 mm**	**0.35 mm**
flange diameter d_f	Coefficient	14.345 mm	0.00008 mm/rpm	−0.00004 mm/rpm	0.00338 min	0.00039 min	−0.12368 mm
	p-value	<5% ✓	<5% ✓	<5% ✓	<5% ✓	<5% ✓	<5% ✓
	Max. effect	**-**	**1.09 mm**	**−0.35 mm**	**0.51 mm**	**0.26 mm**	**−0.25 mm**

The output variable of relative weight loss gives an indication of what percentage of the material is effectively used to manufacture the FSJC and what percentage of the material is removed by the tool contact. Here, too, the feed rate during forming shows a significantly stronger effect compared to the also significant predictors of rotational speed during both pre-rubbing and forming. In line with the results of the undercut, a conflict of objectives in the optimisation of the feed rate during forming can be shown. This should be selected maximally for setting an optimum of the undercut and minimally for the lowest possible weight loss.

Since the shaft diameter of the FSJC is not varied by changing the path geometry in the investigations presented here, this shaft diameter should be constant at one value for all investigation points and independent of the input variables. Due to process-related effects (such as the formation of a built-up cutting edge due to aluminium adhesion), there are significant influences (p-value < 5%) for the variation of the feed rates as well as the material condition on the shaft geometry. Compared to the influences on the process side, the effect of the material condition clearly predominates. When using the hardened (and less ductile) round bar sections in the T66 condition, FSJCs with a larger shaft diameter are manufactured. Here, correspondingly less material is advanced into the flange by the shaping carbide tool. When processing the softer round bar section in the T4 condition, a smaller shaft diameter is set (despite identical tools and path geometry), which may be an indication of stronger aluminium adhesions on the tool. These possible differences in the adhesion tendency must be investigated in future studies and proven with suitable friction tests.

All five predictors investigated have a significant effect on the flange diameter d_f of the FSJC. A high rotational speed as well as a high feed rate during the driving phase lead to a larger flange diameter. This indicates that the pre-rubbing phase (which is omitted in some study points) is important for targeting a high flange diameter. A high rotational speed during the forming of the FSJC as well as the use of semi-finished products from condition T66 results in a smaller flange diameter.

The previously described and explained results of the multivariate regression analysis allow the aluminium FSJC to be influenced in a wide process window. Although pre-rubbing the cross-sectional surface of the semi-finished sections lengthens the entire manufacturing process, it is important for setting a high flange diameter. With a high feed rate during the forming process, two desirable goals can be achieved: maximising the undercut and minimising the process time. At the same time, however, there is still a conflict of objectives in that the weight loss of the FSJC increases with a high feed rate during forming. However, this disadvantage is clearly outweighed by the improved geometry and the reduction of the process time to a few seconds.

4. Conclusions

Based on an extensive experimental plan, this paper presents the potentials and influencing factors of the joining point-dependent manufacturing of different aluminium auxiliary joining elements. For this purpose, in a first step, it is shown that a reproducible manufacturing of uniform Friction Spun Joint Connectors (FSJCs) is possible with the thermomechanical forming process used, considering several series of experiments with four repetition experiments each. This applies both to the geometric parameters considered here (i.e., the undercut and shaft diameter) and the process variable of the maximum tool temperature. This finding is essential both for an industrial application of this process and for further investigations into the variability of the FSJC geometry. The influences of different predictors (influencing variables) on a wide range of values on the geometry of the FSJC as well as on relevant process variables are presented in a second part of this paper. By means of multivariate regression analysis, it can be shown, among other things, that the optimization of the feed rate during the forming of the FSJC significantly reduces the process time and simultaneously optimises the undercut, which is important for the subsequent joining process. Based on the results obtained here, it is important to investigate in future studies whether comparable phenomena can also be demonstrated for other materials under investigation, such as the harder steel C45 E.

Author Contributions: Conceptualisation, T.B. and W.H.; methodology, T.B.; investigation, T.B. and M.H.; writing—original draft preparation, T.B.; writing—review and editing, T.B., M.H. and W.H.; project administration, W.H.; funding acquisition, W.H. All authors have read and agreed to the published version of the manuscript.

Funding: This research was funded by the Deutsche Forschungsgemeinschaft (DFG, German Research Foundation) – TRR 285/2 – 418701707. The authors thank the German Research Foundation for their organisational and financial support.

Data Availability Statement: The data presented in this study are available on request from the corresponding author.

Conflicts of Interest: The authors declare no conflict of interest.

References

1. Giampieri, A.; Ling-Chin, J.; Ma, Z.; Smallbone, A.; Roskilly, A.P. A review of the current automotive manufacturing practice from an energy perspective. *Appl. Energy* **2020**, *261*, 114074. [CrossRef]
2. Milovanoff, A.; Kim, H.C.; de Kleine, R.; Wallington, T.J.; Posen, I.D.; MacLean, H.L. A Dynamic Fleet Model of U.S Light-Duty Vehicle Lightweighting and Associated Greenhouse Gas Emissions from 2016 to 2050. *Environ. Sci. Technol.* **2019**, *53*, 2199–2208. [CrossRef]
3. Buberger, J.; Kersten, A.; Kuder, M.; Eckerle, R.; Weyh, T.; Thiringer, T. Total CO_2-equivalent life-cycle emissions from commercially available passenger cars. *Renew. Sustain. Energy Rev.* **2022**, *159*, 112158. [CrossRef]
4. Ghosh, T.; Kim, H.C.; de Kleine, R.; Wallington, T.J.; Bakshi, B.R. Life cycle energy and greenhouse gas emissions implications of using carbon fiber reinforced polymers in automotive components: Front subframe case study. *Sustain. Mater. Technol.* **2021**, *28*, e00263. [CrossRef]
5. Striewe, J.; Reuter, C.; Sauerland, K.-H.; Tröster, T. Manufacturing and crashworthiness of fabric-reinforced thermoplastic composites. *Thin-Walled Struct.* **2018**, *123*, 501–508. [CrossRef]
6. Galińska, A. Mechanical Joining of Fibre Reinforced Polymer Composites to Metals—A Review. Part I: Bolted Joining. *Polymers* **2020**, *12*, 2252. [CrossRef]

7. Sadeghian, A.; Iqbal, N. A review on dissimilar laser welding of steel-copper, steel-aluminum, aluminum-copper, and steel-nickel for electric vehicle battery manufacturing. *Opt. Laser Technol.* **2022**, *146*, 107595. [CrossRef]
8. Soomro, I.A.; Pedapati, S.R.; Awang, M. A review of advances in resistance spot welding of automotive sheet steels: Emerging methods to improve joint mechanical performance. *Int. J. Adv. Manuf. Technol.* **2022**, *118*, 1335–1366. [CrossRef]
9. Kalyankar, V.; Chudasama, G. On the metallurgical challenges of intermetallic compound in steel/Al dissimilar resistance spot welding: Significance, growth and controlling mechanisms. *Adv. Mater. Process. Technol.* **2023**, 1–33. [CrossRef]
10. Nagatsuka, K.; Xiao, B.; Wu, L.; Nakata, K.; Saeki, S.; Kitamoto, Y.; Iwamoto, Y. Resistance spot welding of metal/carbon-fibre-reinforced plastics and applying silane coupling treatment. *Sci. Technol. Weld. Join.* **2018**, *23*, 181–186. [CrossRef]
11. Xu, H.; Fang, X. Resistance insert spot welding: A new joining method for thermoplastic FRP–steel component. *Weld. World* **2023**, *67*, 1733–1752. [CrossRef]
12. Meschut, G.; Merklein, M.; Brosius, A.; Drummer, D.; Fratini, L.; Füssel, U.; Gude, M.; Homberg, W.; Martins, P.; Bobbert, M.; et al. Review on mechanical joining by plastic deformation. *J. Adv. Join. Process.* **2022**, *5*, 100113. [CrossRef]
13. Mori, K.; Bay, N.; Fratini, L.; Micari, F.; Tekkaya, A.E. Joining by plastic deformation. *CIRP Ann.* **2013**, *62*, 673–694. [CrossRef]
14. Groche, P.; Wohletz, S.; Brenneis, M.; Pabst, C.; Resch, F. Joining by forming—A review on joint mechanisms, applications and future trends. *J. Mater. Process. Technol.* **2014**, *214*, 1972–1994. [CrossRef]
15. Lechner, M.; Kappe, F.; Römisch, D.; Rostek, T.; Wituschek, S. Innovative mechanical joining processes in versatile process chains—Potentials, applications and selection procedures. In Proceedings of the Sheet Metal 2023: 20th International Conference on sheet Metal, Erlangen-Nürnberg, Germany, 2–5 April 2023; Materials Research Forum LLC: Millersville, PA, USA, 2023; pp. 101–108.
16. Popp, J.; Kleffel, T.; Römisch, D.; Papke, T.; Merklein, M.; Drummer, D. Fiber Orientation Mechanism of Continuous Fiber Reinforced Thermoplastics Hybrid Parts Joined with Metallic Pins. *Appl. Compos. Mater.* **2021**, *28*, 951–972. [CrossRef]
17. Siddique, A.; Iqbal, Z.; Nawab, Y.; Shaker, K. A review of joining techniques for thermoplastic composite materials. *J. Thermoplast. Compos. Mater.* **2023**, *36*, 3417–3454. [CrossRef]
18. Martinsen, K.; Hu, S.J.; Carlson, B.E. Joining of dissimilar materials. *CIRP Ann.* **2015**, *64*, 679–699. [CrossRef]
19. Liu, Y.; Zhuang, W.; Luo, Y.; Xie, D.; Mu, W. Joining mechanism and damage of self-piercing riveted joints in carbon fibre reinforced polymer composites and aluminium alloy. *Thin-Walled Struct.* **2023**, *182*, 110233. [CrossRef]
20. Reisgen, U.; Schiebahn, A.; Naumov, A.; Maslennikov, A.; Erofeev, V. Thermo-mechanical model of the friction stir welding process and its application for the aluminium alloy AA5754. In *Mathematical Modelling of Weld Phenomena 12*; Graz University of Technology: Graz, Austria, 2018.
21. Huang, Z.-C.; Huang, G.-H.; Shan, F.-W.; Jiang, Y.-Q.; Zou, Y.-Q.; Nie, X.-Y. Forming Quality and Microstructure Evolution of AA6061-T6 Aluminum Alloy Joint during Flow Drill Screwing Process. *Adv. Eng. Mater.* **2023**, *25*, 2300054. [CrossRef]
22. Altvater, S.; Sikora, S.P.; Siefkes, T. Transition between flow-drill screwing systems considering joining process and joint characteristics. *Adv. Ind. Manuf. Eng.* **2022**, *5*, 100091. [CrossRef]
23. Costas, M.; Morin, D.; Sønstabø, J.K.; Langseth, M. On the effect of pilot holes on the mechanical behaviour of flow-drill screw joints. Experimental tests and mesoscale numerical simulations. *J. Mater. Process. Technol.* **2021**, *294*, 117133. [CrossRef]
24. Aslan, F.; Langlois, L.; Balan, T. Experimental analysis of the flow drill screw driving process. *Int. J. Adv. Manuf. Technol.* **2019**, *104*, 2377–2388. [CrossRef]
25. Kumar Rajak, D.; Pagar, D.D.; Menezes, P.L.; Eyvazian, A. Friction-based welding processes: Friction welding and friction stir welding. *J. Adhes. Sci. Technol.* **2020**, *34*, 2613–2637. [CrossRef]
26. Rana, H.; Patel, V.; Buffa, G.; Fratini, L.; Di Lorenzo, R. Influence of distinct tool pin geometries on aluminum 8090 FSW joint properties. In Proceedings of the Sheet Metal 2023: 20th International Conference on sheet Metal, Erlangen-Nürnberg, Germany, 2–5 April 2023; Materials Research Forum LLC: Millersville, PA, USA, 2023; pp. 195–202.
27. Lertora, E.; Gambaro, C. AA8090 Al-Li Alloy FSW parameters to minimize defects and increase fatigue life. *Int. J. Mater. Form.* **2010**, *3*, 1003–1006. [CrossRef]
28. Heidarzadeh, A. Tensile behavior, microstructure, and substructure of the friction stir welded 70/30 brass joints: RSM, EBSD, and TEM study. *Arch. Civ. Mech. Eng.* **2019**, *19*, 137–146. [CrossRef]
29. Wischer, C.; Wiens, E.; Homberg, W. Joining with versatile joining elements formed by friction spinning. *J. Adv. Join. Process.* **2021**, *3*, 100060. [CrossRef]
30. Wischer, C.; Homberg, W. A contribution on versatile process chains: Joining with adaptive joining elements, formed by friction spinning. *Prod. Eng.* **2022**, *16*, 379–388. [CrossRef]
31. Wischer, C.; Homberg, W. Further Development of an Adaptive Joining Technique Based on Friction Spinning to Produce Pre-Hole-Free Joints. *Key Eng. Mater.* **2022**, *926*, 1468–1478. [CrossRef]